Decorating Graphene Sheets with ZnO Hollow Microspheres using Solvothermal Method

Abqari Luthfi Albert[1,2]*, Shahidan Radiman[2], Wee Siong Chiu[3], Muhammad Azmi Abdul Hamid[2] & Fadhlul Wafi Badrudin[1]

[1]*Physics Department, Centre for Defence Foundation Studies, National Defence University of Malaysia, Sungai Besi Camp, 57000 Kuala Lumpur, Malaysia*

[2]*School of Applied Physics, Faculty of Science and Technology, Universiti Kebangsaan Malaysia, 43600 Bangi, Selangor, Malaysia*

[3]*Low Dimensional Materials Research Center, Department of Physics, Faculty of Science, University of Malaya, 50603 Kuala Lumpur, Malaysia*

**Corresponding authors: albert@upnm.edu.my*

ABSTRACT

Graphene-ZnO microspheres composites were prepared through a facile solvothermal synthesis route at 150 °C for 24 h. The morphological structures of the samples were characterized using Raman spectroscopy, X-ray diffraction (XRD), field emission scanning electron microscopy (FESEM) and transmission electron microscopy (TEM). The analysis revealed that homogeneous microspheres assembling by hexagonal phase wurtzite ZnO nanoparticles were decorated on the graphene sheets via graphene oxide (GO) functional groups. The dimension of the ZnO nanoparticles is approximately 30 nm and the microspheres are hollow. A possible growth mechanism for the formation of ZnO hollow microspheres anchored on the graphene sheets has been proposed. The unique structure of the graphene-ZnO hollow microspheres (G-ZnO(HMs)) composites could have applications in electronics, photonics and medicine.

Keywords: *Graphene, Zinc Oxide, Hollow Sphere, Composites, Solvothermal*

1. Introduction

In recent years, graphene, a single sheet of sp^2-hybridized carbon atoms compacted into a two-dimensional honeycomb lattice, has intrigued enormous research interests. The electrical, mechanical, thermal, and optical characteristics of this carbon allotrope are fascinating [1-7]. Meanwhile, by combining graphene sheets with nanoscale or micron-sized transition metal oxides to create novel hybrid materials, these capabilities can be further enhanced. Various transition metal oxide structures have been anchored to graphene layers in order to achieve exceptional hybrid characteristics [8-19]. Zinc oxide (ZnO) is a type of transition metal oxide that has been extensively studied for a variety of potential applications due to its unique characteristics. With a significant exciton binding energy of 60 MeV at ambient temperature, ZnO is one of the fascinating wide and direct bandgap semiconducting materials. It is a non-toxic, environmentally acceptable, readily available material with a cheap production cost. The multifunctional character of ZnO, which can be altered by altering its morphology and crystallinity, has sparked a lot of attention in the last two decades [20]. ZnO hollow microspheres are of interest in many technological applications such as solar cells [21-23], lithium-ion batteries [24,25], photocatalysis [26-28], sensors [29-31], supercapacitor electrode materials [32,33] and medical [34] because of their low density, high surface area and hollow geometrical shapes.

Hybridisation of graphene and ZnO structures is a viable way to improve their performance far beyond what those materials can achieve on their own [35]. The synergistic impact that occurs between the two building elements is responsible for this extraordinary performance. However, the hybridisation of graphene and ZnO hollow microspheres through a solvothermal synthesis route has rarely been described.

In this study, graphene-zinc oxide hollow microspheres (G-ZnO(HMs)) composites were prepared using a solvothermal processing method. This one-pot synthesis method is simple, efficient, and does not involve the use of any reducing or oxidising agents. On the surface of graphene, in situ growth of ZnO resulted in uniformly adorned hollow microspheres. The morphological properties of G-ZnO (HMs) composites were thoroughly investigated.

2. Experimental

2.1 Materials

Commercially available graphene oxide (GO, 99 wt%) powder was acquired from Cheap Tubes Inc. (Grafton, US). Merck and HmbG Chemicals provided zinc acetate dihydrate (Zn(CH3COO)2.2H2O, 99.5 %) and absolute ethanol, respectively. All of the reagents were used exactly as they were received, with no further purification, and distilled water was used throughout the sample preparation process.

2.2 Solvothermal preparation of G-ZnO(HMs) composites

GO powder was dissolved in absolute ethanol to achieve a concentration of 1 mg/ml of GO and stirred continuously for 30 minutes. Subsequently, 5.0 mM of $Zn(CH_3COO)_2.2H_2O$ was added and the mixture suspension was sonicated for 30 minutes to obtain a homogeneous solution. The suspension was then transferred into a Teflon-lined stainless autoclave. The autoclave was sealed and maintained in the oven at 150 °C for 24 hours. After cooling the autoclave to room temperature naturally, the black precipitates were separated by centrifugation, and washed with distilled water and absolute ethanol repeatedly. The pure G-ZnO(HMs) composites powder was dried in the oven at 60 °C for 8 hours. For comparison purpose, a control experiment was performed without adding zinc precursor and the product was labelled as rGS.

2.3 Physical characterisation of G-ZnO(HMs) composites

The X-ray diffraction (XRD) spectra on powdered samples was collected via a Bruker D8 Advance 9 Position diffractometer using Cu K-α radiation (λ = 0.15406 nm) to determine the crystalline phase of the samples. The disordering of the formed carbon was examined using Raman spectroscopy (Renishaw inVia system with a laser of 25 mV at 532 nm). A field emission scanning electron microscope (FESEM, Zeiss Merlin) and a transmission electron microscope (TEM, Philips CM12) were used to analyse the structural morphology of G-ZnO(HMs) composites.

3. Results and discussion

3.1 Physical characteristics

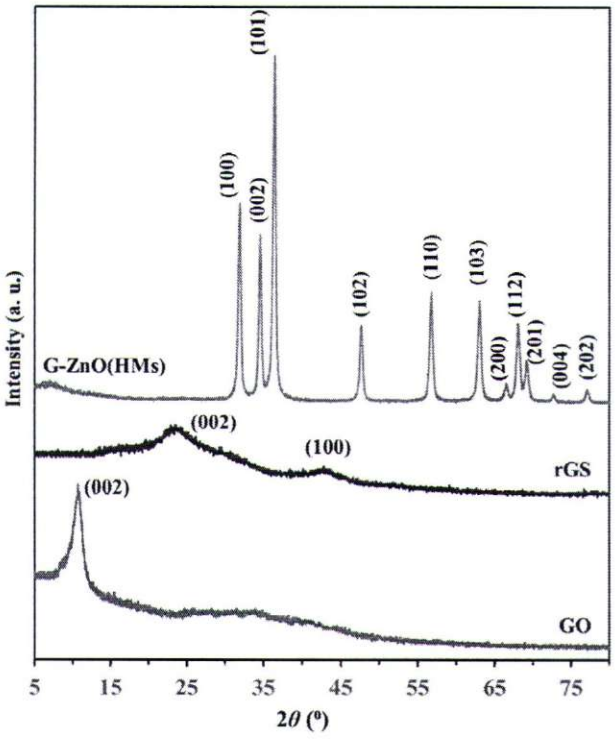

Fig. 1. XRD-spectra for GO, rGS and G-ZnO(HMs) composite.

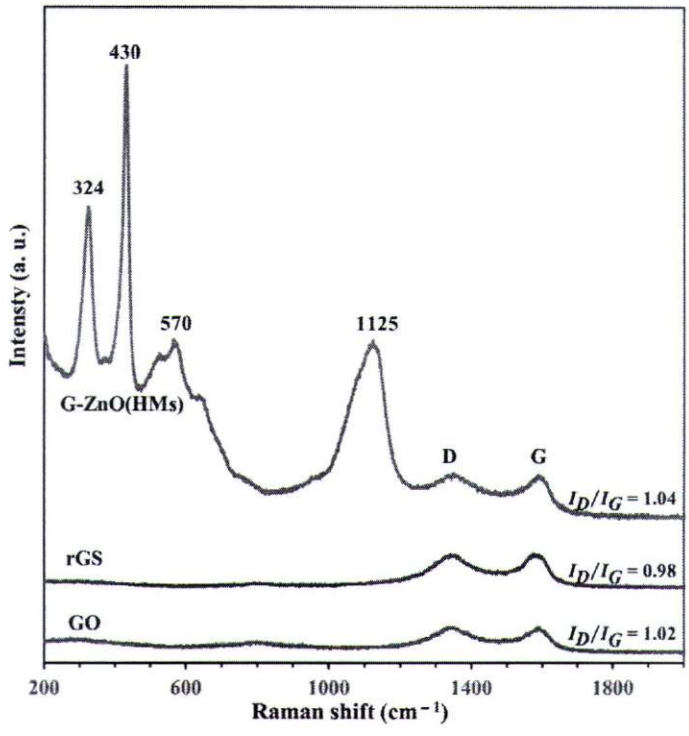

Fig. 2. Raman spectra for GO, rGS and G-ZnO(HMs) composite.

The XRD patterns of the GO, rGS and G-ZnO(HMs) composite are shown in Fig. 1. The peak emerging at approximately 11.0° in the GO pattern is associated with the presence of oxygenated functional groups attached to the basal planes and edges of carbon sheets [36]. Meanwhile, the appearance of small bumps at 23.5° and 42.8° in the rGS pattern, which indicates the removal of a large number of oxygen-containing groups and the formation of much more disordered graphene sheets, verifies the reduction of GO to rGS, or reduced graphene oxide [36,37]. The diffraction peaks of G-ZnO(HMs) composites at around 31.9°, 34.5°, 36.3°, 47.6°, 56.7°, 62.9°, 66.4°, 67.9°, 69.3°, 72.5°, and 77.0° agree well with the hexagonal phase wurtzite of the ZnO structure, which is in accordance with the reference pattern JPCDS 36-1451 [38]. No characteristic peaks of any impurities were detected, suggesting that high-quality ZnO nanoparticles were synthesized. The sharp and intense diffraction peaks are highly remarkable, indicating the formation of a well-crystalline structure of ZnO nanoparticles on the graphene surface. The absence of the GO peak indicates that GO was completely reduced throughout the hybridisation process. Due to the extensive formation of ZnO and the relatively low amount of rGS, no diffraction peak of rGS can be observed in the composites [37,39].

The presence of both carbon and ZnO in the structure of the prepared G-ZnO(HMs) composite can be confirmed from the Raman spectra. As shown in Fig. 2, the characteristic Raman peaks of G-ZnO(HMs) composite exhibit D and G bands at around 1347 cm^{-1} and 1589 cm^{-1}, respectively. The G band provides useful information on in-plane stretching vibrations of symmetric sp^2 C–C bonds, while the D band is associated with the disturbance of the hexagonal graphitic lattice [40, 41]. Compared with rGS, the D and G band in G-ZnO(HMs) composites were blue-shifted by 5 cm^{-1} and 14 cm^{-1}, respectively. These shifts are assigned to the chemical interaction between ZnO and rGS, which suggests that the electronic structure of the rGS could be modified by contacting with ZnO

nanoparticles [36]. The intensity ratio of D band to G band, I_D/I_G can be used to measure the relative defect content in the sp^2 carbon lattice [42]. The calculated I_D/I_G ratios for GO, rGS, and the G-ZnO (HMs) composite are 1.02, 0.98, and 1.04, respectively. The I_D/I_G ratio of rGS is smaller than that of GO, which suggests an increase in the average size of the in-plane sp^2 domains upon reduction of the GO. The relatively high I_D/I_G ratio for GO is contributed by the presence of oxygenated functional groups on both sides and edges of the GO sheets [43]. However, the G-ZnO(HMs) composite exhibits the highest I_D/I_G ratio due to the increasing disorder of sp^2 domains contributed by the presence of ZnO nanoparticles on the graphene sheets. The G-ZnO(HMs) composite curves displayed four distinctive Raman vibration modes centred at 324 cm^{-1}, 430 cm^{-1}, 570 cm^{-1} and 1125 cm^{-1}, which are referred to the ZnO spectrum. The edge at about 324 cm^{-1} has been assigned to the second order Raman scattering (E_2 (high)–E_2 (low) mode) and arises from zone-boundary phonon of hexagonal ZnO [44]. The intense peak at 430 cm^{-1} corresponds to the nonpolar optical phonon E_2 (high) mode, which is known as Raman active optical phonon mode and is related to the motion of oxygen atoms [41,45]. The presence of the E_2 (high) mode in the composite samples, which is the characteristic of wurtzite hexagonal phase ZnO is consistent with the above XRD analysis. The peak at 570 cm^{-1} is assigned to E_1 longitudinal optical (E_1 (LO)) mode, attributed to oxygen deficiency defects in ZnO [44]. The broad band at 1125 cm^{-1} is due to the multiple-phonon scattering processes ($2A_1$ (LO), $2E_1$ (LO) and 2LO mode), characteristic of the II-IV semiconductor [41,46].

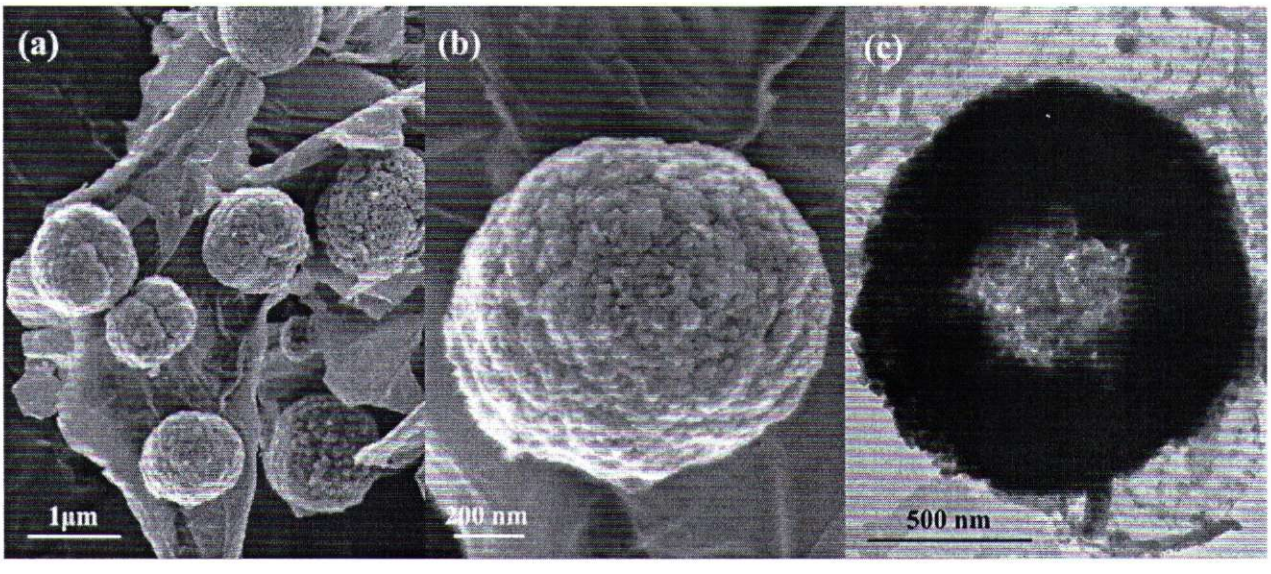

Fig. 3. FESEM images of (a) G-ZnO(HMs) composite, and (b) G-ZnO(HMs) composite with high-magnification; (c) TEM images of a single ZnO hollow sphere.

The surface morphology of the as-prepared G-ZnO(HMs) composite was investigated using FESEM. The graphene structure was found to be anchored by homogenous ZnO hollow microspheres (Fig. 3(a)). The diameter of the microspheres ranged from 800 to 1200 nm and they were evenly dispersed on the graphene surface. The microspheres are composed of ZnO nanoparticles about 30 nm in diameter, as shown in the high-magnification image (Fig. 3(b)), which is consistent with the above XRD data. The structure of the ZnO hollow microspheres formed on the graphene's surface was also determined via TEM analysis. The hollow interiors of the unique ZnO microspheres are clearly confirmed by the fact that the centre region of the microsphere is lighter than the edge (Fig. 3(c)).

3.2 *Formation mechanism of G-ZnO(HMs) composite*

The formation mechanism of ZnO hollow microspheres on graphene sheet is shown in Fig. 4. GO contains large amounts of epoxide, hydroxyl and carboxyl acid reactive groups on its surface and edges. These functional groups immobilize Zn^{2+} ions through C–O–Zn bonds, thereby through condensation reaction, enabling Zn^{2+} to be connected to these nucleation sites and ZnO quantum dots grown on graphene sheet *via* normal ionic bonds [47]. The high temperature inside the autoclave stimulates the nucleation and subsequent growth of ZnO quantum dots to form nanoparticle. Simultaneously, due to the high temperature condition, ethanol can effectively remove most of the oxygen-functional groups and restore the conjugated network of graphitic lattice of GO, resulting in the rGS [48]. The ZnO nanoparticles preferentially aggregate and self-assemble into metastable spheres by the well-known growth mechanism of "oriented attachment" to minimize the total surface energy [49]. On a prolonged solvothermal process, the inner phase of metastable ZnO spheres with higher energy will move to stable outer surface through Ostwald ripening, resulting in the hollow structure.

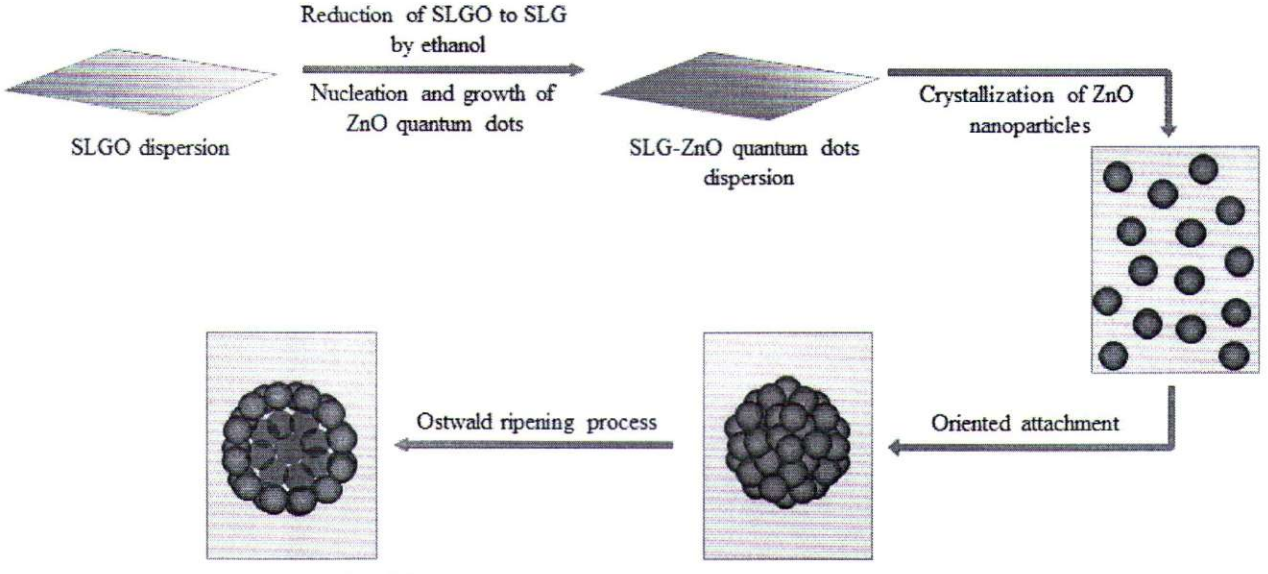

Fig. 4. Schematic of the formation mechanism of ZnO hollow spheres on SLG sheet.

Conclusions

The G-ZnO(HMs) composite was synthesized via a simple, facile and scalable solvothermal method at 150 °C for 24 h without using any reducing or oxidizing agent. The analysis revealed that homogeneous microspheres assembling by hexagonal phase wurtzite ZnO nanoparticles were decorated on the graphene sheets via graphene oxide (GO) functional groups. The dimension of the ZnO nanoparticles is approximately 30 nm and the microspheres are hollow.

Acknowledgements

Financial support from the Universiti Pertahanan Nasional Malaysia (UPNM) Geran Penyelidikan Jangka Pendek (UPNM/2020/GPJP/SG/6) and the Ministry of Higher Education (MOHE) of Malaysia are gratefully acknowledged. The authors also express profound gratitude to the Centre for Research and Instrumentation (CRIM), Universiti Kebangsaan Malaysia (UKM), for access to its analytical equipment.

References

[1] S.K. Abdel-Aal, A.S. Abdel-Rahman, Graphene influence on the structure, magnetic, and optical properties of rare-earth perovskite, J Nanopart Res 22 (2020) 267.

[2] G. Jing, Z. Ye, J. Wu, S. Wang, X. Cheng, V. Strokova, V. Nelyubova, Introducing reduced graphene oxide to enhance the thermal properties of cement composites, Cem Concr Compos 109 (2020) 103559.

[3] N. Khobragade, K. Sikdar, B. Kumar, S. Bera, D. Roy, Mechanical and electrical properties of copper-graphene nanocomposite fabricated by high pressure torsion, J. Alloys Compd 776 (2019) 123-132.

[4] R. Aradhana, S. Mohanty, S.K. Nayak, Comparison of mechanical, electrical and thermal properties in graphene oxide and reduced graphene oxide filled epoxy nanocomposite adhesives, Polymer 141 (2018) 109-123.

[5] S. Bai, L. Jiang, N. Xu, M. Jin, S. Jiang, Enhancement of mechanical and electrical properties of graphene/cement composite due to improved dispersion of graphene by addition of silica fume, Constr Build Mater. 164 (2018) 433-441.

[6] K. Chu, X.-h. Wang, Y.-b. Li, D.-j. Huang, Z.-r. Geng, X.-l. Zhao, H. Liu, H. Zhang, Thermal properties of graphene/metal composites with aligned graphene, Mater. Des 140 (2018) 85-94.

[7] S. Prabhu, M. Pudukudy, S. Sohila, S. Harish, M. Navaneethan, D. Navaneethan, R. Ramesh, Y. Hayakawa, Synthesis, structural and optical properties of ZnO spindle/reduced graphene oxide composites with enhanced photocatalytic activity under visible light irradiation, Opt. Mater. 79 (2018) 186-195.

[8] Z. Wang, Z. Jia, Q. Li, X. Zhang, W. Sun, J. Sun, B. Liu, B. Ha, The enhanced NO_2 sensing properties of SnO_2 nanoparticles/reduced graphene oxide composite, J. Colloid Interface Sci. 537 (2019) 228-237.

[9] S. Zuo, D. Li, Z. Wu, Y. Sun, Q. Lu, F. Wang, R. Zhuo, D. Yan, J. Wang, P. Yan, SnO_2/graphene oxide composite material with high rate performance applied in lithium storage capacity, Electrochim. Acta 264 (2018) 61-68.

[10] H.E. Marouazi, P. Jiménez-Calvo, E. Breniaux, C. Colbeau-Justin, I. Janowska, V. Keller, Few Layer Graphene/TiO_2 Composites for Enhanced Solar-Driven H_2 Production from Methanol, ACS Sustain. Chem. Eng. 9 (2021) 3633-3646.

[11] M. Ruidíaz-Martínez, M.A. Álvarez, M.V.López-Ramón, G. Cruz-Quesada, J. Rivera-Utrilla, M. Sánchez-Polo, Hydrothermal Synthesis of rGO-TiO_2 Composites as High-Performance UV Photocatalysts for Ethylparaben Degradation, Catalyst 10 (2020) 520.

[12] J. Azuaje, A. Rama, A. Mallo-Abreu, M.G. Boado, M. Majellaro, C.R. Tubío, R. Prieto, X. García-Mera, F. Guitian, E. Sotelo, Alvaro Gil, Catalytic performance of a metal-free graphene oxide-Al_2O_3 composite assembled by 3D printing, J. Eur. Ceram. Soc. 41 (2021) 1399-1406.

[13] J. Li, J. Ji, J. Chen, W. Zhang, Synthesis of TiO_2/reduced graphene oxide–$Al2O_3$ composites and their advanced properties for photocatalysis, J. Nanoparticle Res. 22 (2020) 224.

[14] X. Hu, Y. Yu, S. Ren, N. Lin, Y. Wang, J. Zhou, Highly efficient removal of phenol from aqueous solutions using graphene oxide/Al_2O_3 composite membrane, J. Porous Mater. 25 (2018) 719-726.

[15] K.-Y. Chen, S. Gupta, N.-H. Tai, Reduced graphene oxide/Fe_2O_3 hollow microspheres coated sponges for flexible electromagnetic interference shielding composites, Compos. Commun. 23 (2021) 100572.

[16] F. Wang, X. Li, Z. Chen, W. Yu, K.P. Loh, B. Zhong, Y. Shi, Q.-H. Xu, Efficient low-frequency microwave absorption and solar evaporation properties of γ-Fe_2O_3 nanocubes/graphene composites, Chem. Eng. J. 405 (2021) 126676.

[17] Z. Zhou, C. Ding, W. Peng, Y. Li, F. Zhang, X. Fan, One-step fabrication of two-dimensional hierarchical Mn_2O_3@graphene composite as high-performance anode materials for lithium ion batteries, J. Mater. Sci. Technol. 80 (2021) 13-19.

[18] H. Han, Q.A. Sial, S.S. Kalanur, H. Seo, Binder assisted self-assembly of graphene oxide/Mn_2O_3 nanocomposite electrode on Ni foam for efficient supercapacitor application, Ceram. Int. 46 (2020) 15631-15637.

[19] D.R. Rout, S. Chaurasia, H.M. Jena, Enhanced photocatalytic degradation of malachite green using manganese oxide doped graphene oxide/zinc oxide (GO-ZnO/Mn_2O_3) ternary composite under sunlight irradiation, J. Environ. Manage. 318 (2022) 115449.

[20] M.K. Kavitha, H. John, P. Gopinath, R. Philip, Synthesis of reduced graphene oxide-ZnO hybrid with enhanced optical limiting properties, J. Mater. Chem. C 1 (2013) 3669-3676.

[21] L. Yu, W. Hao, Z. Li, X. Ren, H. Yang, H. Ma, Synthesis of ZnO core/shell hollow microspheres to boost light harvesting capability in quantum dots-sensitized solar cell, Chem. Phys. Lett. 764 (2021) 138283.

[22] A. Banik, M.S. Ansari, M. Qureshi, Efficient Energy Harvesting in SnO_2-Based Dye Sensitized Solar Cells Utilizing Nano-Amassed Mesoporous Zinc Oxide Hollow Microspheres as Synergy Boosters, ACS Omega 3 (2018) 14482-14493.

[23] L. Wang, C. Ma, X. Ru, Z. Guo, D. Wu, S. Zhang, G. Yu, Y. Hu, J. Wang, Facile synthesis of ZnO hollow microspheres and their high performance in photocatalytic degradation and dye sensitized solar cells, J. Alloys Compd. 647 (2015) 57-62.

[24] G. Wua, Z. Jiaa, Y. Cheng, H. Zhang, X. Zhou, H. Wu, Easy synthesis of multi-shelled ZnO hollow spheres and their conversion into hedgehog-like ZnO hollow spheres with superior rate performance for lithium ion batteries, Appl. Surf. Sci. 464 (2019) 472-478.

[25] S.-C. Weng, S. Brahma, C.-C. Chang, J.-L. Huang, Synthesis of self-assembled Hollow-Sphere ZnO/rGO Nanocomposite as Anode Materials for Lithium-Ion Batteries, Int. J. Electrochem. Sci. 14 (2019) 3727-3739.

[26] L. Zhou, Z. Han, G.-D. Li, Z. Zha, Template-free synthesis and photocatalytic activity of hierarchical hollow ZnO microspheres composed of radially aligned nanorods, J. Phys. Chem. Solids 148 (2021) 109719.

[27] C. Chen, X. Liu, Q. Fang, X. Chen, T. Liu, M. Zhan, Self-assembly synthesis of CuO/ZnO hollow microspheres and their photocatalytic performance under natural sunlight, Vacuum 174 (2020) 109198.

[28] M.R. Hernández, A.d.L. Santillán, E.d.C. Ortiz, S.F. Tavizón, I. Moggio, E. Arias, C.A. Gallardo-Vega, J.A.M. Silva, E.D. Barriga-Castro, Hollow ZnO microspheres functionalized with electrochemical graphene oxide for the photodegradation of salicylic acid, RSC Adv. 9 (2019) 6965-6972.

[29] H. Wang, Y. Yang, T. Xie, Y. Lin, Highly Sensitive and Selective HCHO Sensor Based on Co Doped ZnO Hollow Microspheres Activated by UV Light, IEEE Sens. J. 21(6) (2021) 7558-7564.

[30] S. Wang, G. Qiao, X. Chen, X. Wang, H. Cui, Synthesis of ZnO Hollow Microspheres and Analysis of Their Gas Sensing Properties for *n*-Butanol, Crystals 10 (2020) 1010.

[31] M. Xiao, Y. Li, B. Zhang, G. Sun, Z. Zhang, Synthesis of g-C3N4-Decorated ZnO Porous Hollow Microspheres for Room-Temperature Detection of CH4 under UV-Light Illumination, Nanomaterials 9 (2019) 1507.

[32] A.L. Albert, S. Radiman, M.A.A. Hamid, M.F.Y.M. Hanappi, Physical and Electrochemical Properties of Graphene Decorated with ZnO Hollow Spheres for Supercapacitor Applications, Key Engineering Materials 908 (2022) 284-292.

[33] G.-C. Li, P.-F. Liu, R. Liu, M. Liu, K. Tao, S.-R, Zhu, M.-K. Wu, F.-Y. Yia, L. Han, MOF-derived hierarchical double-shelled NiO/ZnO hollow spheres for high-performance supercapacitor, Dalton Trans. 45(34) (2016) 13311-13316.

[34] N. Puvvada, S. Rajput, B.N.P. Kumar, S. Sarkar, S. Konar, K.R. Brunt, R.R. Rao, A. Mazumdar, S.K. Das, R. Basu, P.B. Fisher M. Mandal, A. Pathak, Novel ZnO hollow-nanocarriers containing *paclitaxel* targeting folate-receptors in a malignant pH-microenvironment for effective monitoring and promoting breast tumor regression, Sci. Rep. 5 (2015) 11760.

[35] A. Ramadoss, S.J. Kim, Improved activity of a graphene-TiO_2 electrode in an electrochemical supercapacitor, Carbon 63 (2013) 434-445.

[36] F.S. Omar, H.N. Ming, S.M. Hafiz, L.H. Ngee, Microwave Synthesis of Zinc Oxide/Reduced Graphene Oxide Hybrid for Adsorption-Photocatalysis Application, Int. J. Photoenergy 2014 (2014) 1-8.

[37] T. Lv, L. Pan, X. Liu, T. Lu, G, Zhu, Z. Sun, Enhanced photocatalytic degradation of methylene blue by ZnO-reduced graphene oxide composite synthesized via microwave-assisted reaction, J. Alloys Compd. 509 (2011) 10086-10091.

[38] Y.-M. Lu, C.-F. Tseng, B.-Y. Lan, C.-F. Hsieh, Fabrication of Graphene/Zinc Oxide Nano-Heterostructure for Hydrogen Sensing, Materials 14 (2021) 6943.

[39] J. Qina, X. Zhang, C.Yang, M. Cao, M. Ma, R. Liu, ZnO microspheres-reduced graphene oxide nanocomposite for photocatalytic degradation of methylene blue dye, Appl. Surf. Sci. 392 (2017) 196-203.

[40] F.S. Ghoreishi, V. Ahmadi, M. Samadpour, Improved performance of CdS/CdSe quantum dots sensitized solar cell by incorporation of ZnO nanoparticles/reduced graphene oxide nanocomposite as photoelectrode, J. Power Sources 271 (2014) 195-202.

[41] S.S. Low, H.-S. Loh, J.S. Boey, P.S. Khiew, W.S. Chiu, M.T.T. Tan, Sensitivity enhancement of graphene/zinc oxide nanocomposite-based electrochemical impedance genosensor for single stranded RNA detection, Biosens. Bioelectron 94 (2017) 365-373.

[42] J. Rodrigues, J. Zanoni, G. Gaspar, A.J.S. Fernandes, A.F. Carvalho, N.F. Santos, T. Monteiro, F.M. Costa, ZnO decorated laser-induced graphene produced by direct laser scribing, Nanoscale Adv. 1 (2019) 3252-3268.

[43] S.P. Lim, N. M. Huang, H. N. Lim, Solvothermal synthesis of SnO_2/graphene nanocomposites for supercapacitor application, Ceram. Int. **39** (2013) 6647-6655.

[44] P. Kumar, V. Singh, V. Sharma, G. Rana, H.K. Malik, K. Asokan, Investigation of phase segregation in yttrium doped zinc oxide, Ceram. Int. 41 (2015) 6734-6739.

[45] D.H. Xu, W.Z. Shen, Cu-Doped ZnO Hemispherical Shell Structures: Synthesis & Room-Temperature Ferromagnetism Properties, J. Phys. Chem. C 116(24) (2012) 13368-13373.

[46] D.A. Guzmán-Embús, M.O. Cardozo, C. Vargas-Hernández, Genomic DNA characterization of pork spleen by Raman spectroscopy, J. Appl. Phys. 114 (2013) 194704: 1-8.

[47] A. Tayyebi, M. outokesh, M. Tayebi, A. Shafikhani, S.S. Şengör, ZnO quantum dots-graphene composites: Formation mechanism and enhanced photocatalytic activity for degradation of methyl orange dye, J. Alloys Compd. 663 (2016) 738-749.

[48] Z.-g. Wang, P.-j. Li, Y.-f. Chen, J.-r. He, B.-j. Zheng, J.-b. Liu, F. Qi, The green synthesis of reduced graphene oxide by the ethanol-thermal reaction and its electrical properties, Mater. Lett. 116 (2014) 416-419.

[49] C.-X. He, B.-X. Lei, Y.-F. Wang, C.-Y. Su, Y.-P. Fang, D.-B. Kuang, Sonochemical preparation of Hierarchical ZnO Hollow spheres for efficient dye-sensitized cells, Chem. Eur. J. 16 (2010) 8757-8761.